J Mater Sci (2008) 43:6094–6098
DOI 10.1007/s10853-008-2949-7

Spectroscopic and quantum chemical investigation of the $4Bi_2O_3 \cdot B_2O_3$ glass structure

S. Rada · E. Culea · V. Rus

Received: 16 April 2008 / Accepted: 12 August 2008 / Published online: 4 September 2008

Abstract The structural properties of the $4Bi_2O_3 \cdot B_2O_3$ glass were investigated by FT-IR spectroscopy and quantum chemical calculations. The main results reveal that the coordination polyhedrons of the bismuth ion from the $[BiO_6]$ structural units and of the boron ion from the $[BO_4]$ groups are irregular. Accordingly, the $[BiO_6]$ and $[BO_4]$ structural units in the studied glass matrix have a complex structural role that makes possible the formation of the vitreous system.

Introduction

Glasses formed with heavy metal ions have received significant attention because of their interesting optical applications [1, 2]. The interest in heavy metal oxide glasses is due to their long infrared cut-off and optical nonlinearity [1, 3]. Bismuth based oxide glasses attracted the scientific community due to their important applications in the field of glass ceramics, thermal and mechanical sensors, reflecting windows [4].

Despite the fact that Bi_2O_3 is not a classical glass former, due to high polarizability and small field strength of Bi^{+3} ions, in the presence of conventional glass formers (such as B_2O_3, PbO, P_2O_5, V_2O_5 [5–9]) it may build a glass network of $[BiO_n]$ ($n = 3, 6$) pyramids [10, 11]. However, the structural role played by Bi_2O_3 in glasses is complicated and poorly understood. This is because the $[BiO_n]$ polyhedra are highly distorted due to the lone pair electrons. Several techniques have been employed in an attempt to identify the local environment of the different elements in bismuthate glasses. X-ray and infrared studies have shown that Bi^{+3} ions participate in the glass network structure above 45 mol% Bi_2O_3 [12]. The addition of Li, Zn, Fe oxides [13–15] results in large glass formation domain.

On the other hand, the structural origins of glassy materials are very important in science today. Semiempirical calculations of the pentaborate clusters that are the basic structural units of the alkali-borate glasses were described in previous papers [16, 17]. Other quantum chemical studies deal with the structure of some silica glasses [18].

Quantum chemistry uses a variety of approaches to approximate the solution of the Schrodinger equation for the system of interest. High level structural modeling methods, both ab initio and DFT, take into account all the electrons in the system. Semiempirical methods use some parameters derived from experimental works and deal only with valence electrons. In all cases, optimized structures are calculated by varying the geometrical parameters until an energy minimum is found.

The main objectives of the present work were to study the structural properties of the boro–bismuthate glasses based on experimental measurements and theoretical models. We attempt to illuminate structural aspects of the $4Bi_2O_3 \cdot B_2O_3$ glass system. By combining calculated vibrational spectra for different clusters, which can form the continuous random network of the glass, with experimental spectrum we aim to define and understand the structure of the $4Bi_2O_3 \cdot B_2O_3$ borate-bismuthate glass network.

Experimental

The $4Bi_2O_3 \cdot B_2O_3$ glass system was obtained from homogenized mixtures of Bi_2O_3 and H_3BO_3 reagents of p.a

S. Rada (✉) · E. Culea · V. Rus
Department of Physics, Technical University of Cluj-Napoca, 400641 Cluj-Napoca, Romania
e-mail: Simona.Rada@phys.utcluj.ro

purity grade by melting at 1200 °C for 20 min in corundum crucibles in an electric furnace. The melts were quenched to room temperature.

The structure of the glasses was investigated by infrared spectroscopy using the KBr pellet technique. The IR spectra were recorded in the 400–1600 cm^{-1} range using a JASCO FTIR 6200 spectrometer.

The starting structures have been built up using the graphical interface of Spartan'04 [19] and preoptimized by molecular mechanics. Optimizations were continued ab initio (HF/LanL2DZ/ECP) and at DFT (B3BW91/CEP-4G/ECP) level using the Gaussian'98 package of programs [20]. For bismuth atoms the effective core potential (ECP) proposed by Hay and Wadt [21] has been adopted together with the associated basic set. The same ECP has been tested in the framework of DFT by carrying out B3PW91 calculations.

It should be noticed that only the broken bonds at the model boundary were terminated by hydrogen atoms. The positions of boundary atoms were frozen during a calculation and the coordinates of internal atoms were optimized to model the active fragment flexibility and its incorporation into the bulk.

Frequency analysis followed all optimizations to establish the nature of the stationary points found, so that all the structures reported in this study are genuine minima on the potential energy surface at this level of theory, without any imaginary frequencies. Accordingly, frequency calculations were performed to ensure that the stationary points were minima and to calculate infrared (IR) spectra. Calculated IR frequencies and intensities were transformed via the SWizard program [22] into simulated IR spectra using Lorentzian functions with half-widths of 15 cm^{-1}.

The fully optimized models obtained by performing ab initio calculations were used to compute the density of state (DOS) and crystal orbital overlap population (COOP) using the BICON-CEDIT package [23].

Results and discussion

The FT-IR spectra of crystalline H_3BO_3 and Bi_2O_3 samples are reported in Fig. 1a and b. As expected, the widths of the absorption bands of these samples are smaller and the peaks intensities are higher than those of the glass samples. In the spectra of the H_3BO_3 crystal, the strong absorption bands are located at ~546, ~647, ~800, and ~1194 cm^{-1}. These infrared absorption bands can be assigned to the B–O–B bending vibrations (~647 cm^{-1}), the [BO_3] triangular unit vibrations (~800 cm^{-1}), and to the B–O bonds from isolated pyroborate groups (~1194 cm^{-1}) [24]. Some authors [25] suggested that the simultaneous

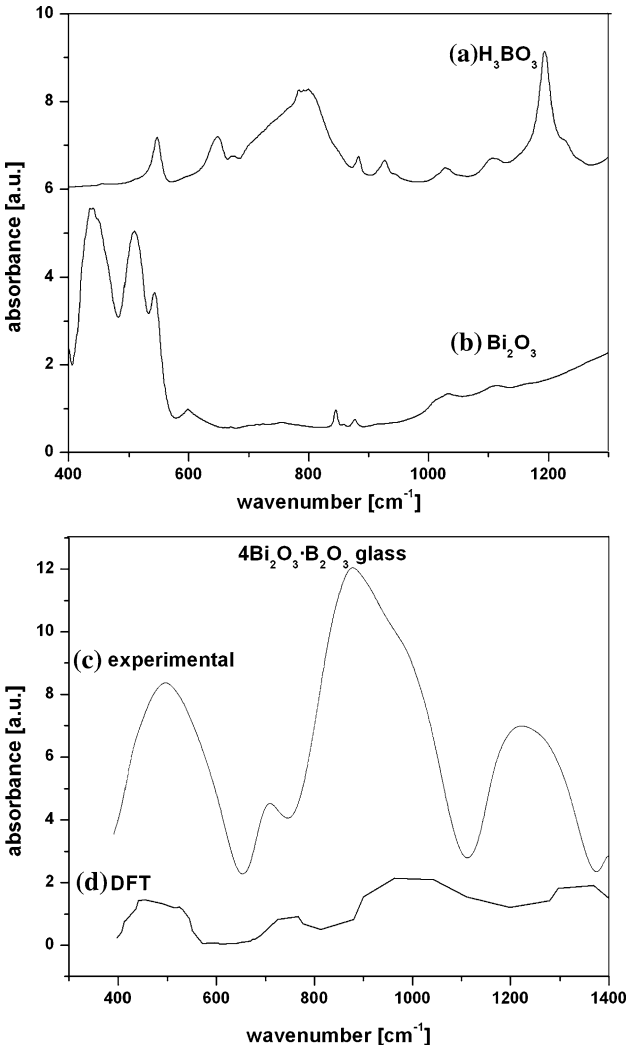

Fig. 1 Experimental FT-IR spectrum of the H_3BO_3 (a) and Bi_2O_3 (b) reference crystals, of the $4Bi_2O_3 \cdot B_2O_3$ glass (c) and of the simulated IR spectrum using Lorentzian functions of the model (d)

occurrence of the bands around ~930, ~770, ~650, and ~550 cm^{-1} is indicative of the presence of pentaborate structural groups.

The infrared spectrum of the crystalline Bi_2O_3 in the small wavenumber region, 400–880 cm^{-1}, presents distinguished IR bands and shoulders located at ~435, ~507, and ~542 cm^{-1} that can be attributed to the Bi–O–Bi vibrations [26].

An evidence for the existence of the [BiO_3] polyhedra is the appearance of a band located around ~840 cm^{-1} in our spectra [27, 28].

The following bands are present in the spectra of the glasses as shown in Fig. 1c: ~496, ~711, ~877, ~1222 cm^{-1}. The infrared band that appears at ~877 cm^{-1} is attributed to the [BO_3] triangular unit vibrations [10]. The band from ~1222 cm^{-1} was assigned to the stretching of the terminal B–O bonds of the pyroborate groups [29]. The

[BO_4] vibrations are observable between ~900 and ~1100 cm^{-1} [30].

As we mentioned for the $4Bi_2O_3 \cdot B_2O_3$ glass, the Bi^{+3} cations are usually incorporated in the glass network as deformed [BiO_6] octahedral and [BiO_3] pyramidal units. The appearance of a breathing vibration of rings containing [BO_3] triangles and [BO_4] tetrahedral structural units as a very small band around ~785 cm^{-1} confirms our assumption that the boron atoms from the glass are three and four coordinated [31].

These data were used in the present research to compute a possible structural model of the $4Bi_2O_3 \cdot B_2O_3$ boro–bismuthate glass. Similar methodology has previously been reported in the study of other glasses [9, 24, 25, 32–34]. In general, good similarities were found between the theoretically calculated Bi–O (2.02–2.11 Å) and B–O (1.47–1.51 Å) bond lengths from the proposed mechanical-quantum models and the experimental values (Fig. 2). Instead of this, several distances are slowly diversified. Thus, in Fig. 2a (model I) a larger distance was found for the Bi–O bond length (3.19 Å) from [BiO_6] unit. This fact was previously reported for the bismuth borate compounds with irregular coordination polyhedra [24, 25]. The investigated model II (Fig. 2b) shows diverse B–O bond lengths (1.52; 1.58; 1.65, and 1.68 Å) from the [BO_4] units suggesting that the [BO_4] structural groups are distorted.

The Bi–O bond distance (3.19 Å) is longer than the Bi–O covalent bond (2.22 Å) but significantly shorter than the sum of the Van der Waals radii (3.52 Å) implying a cation–anion electrostatic interaction with this one. In the model II the long B–O distances are longer than the covalent B–O bond distances (1.51 Å) but shorter than the sum of the Van der Waals radii (3.52 Å). This leads to a much more unsymmetrical coordination of the model II in the vicinity of [BO_4] structural units.

The most stable model is the first one ($E = -42.7145$ au/atom) because the total energy/atom is bigger in absolute value than that of the second model ($E = -8.3218$ au/atom). The coordination polyhedra of the bismuth ion from the [BiO_6] structural units and of the boron ion from [BO_4] structural groups are irregular and the thermodynamic stability of the model increases when the [BiO_6] octahedral units are more distorted.

We mention that the two studied models describing the local disorder in $4Bi_2O_3 \cdot B_2O_3$ glasses are highly possible but are not unique. However, by using other methods than the HF(LanL2DZ/ECP) or DFT (B3BW91/CEP-4G/ECP) utilized in the present paper, the results concerning the Bi–O and B–O bonds length will not change significantly.

Accordingly, these structural models show a very complex behavior and their stabilization can be achieved by several metallic cations [32] or the adequate arranging of these cations into the vitreous network.

The frequencies and relative intensities of the stretching and bending vibrations of the structural groups from the studied models are presented in Fig. 1d. The calculated absorption spectrum of the proposed model is in good agreement with the experimental absorption data.

To understand the electronic nature of this material, we have explored the density of states (DOS) designed for the atomic valence orbitals of bismuth, oxygen, and boron. In Figs. 3a and 4 are plotted total, partial DOS, and IDOS (the integration of the density of state) diagrams indicating that the system has a metallic behavior in the vicinity of the Fermi level. The dashed horizontal line represents the Fermi level, E_F at −11.2301 eV.

The region under the Fermi level has contributions from the O (2s, 2p) derived states and an admixture of the Bi (6s, 6p) and B (2s, 2p) orbitals. The conduction bands consist of a mixture of the B(2s, 2p), Bi(6s, 6p), and O(2p) derived states.

The oxygen projection shows a sharp peak below the Fermi level, at about −26.23 eV. This peak can be ascribed to the O(2s) orbitals. Note that the location of this peak is relatively far away from the Fermi level (at about 15 eV below the Fermi level). We mention that such low values of the O(2s) states were previously reported for some

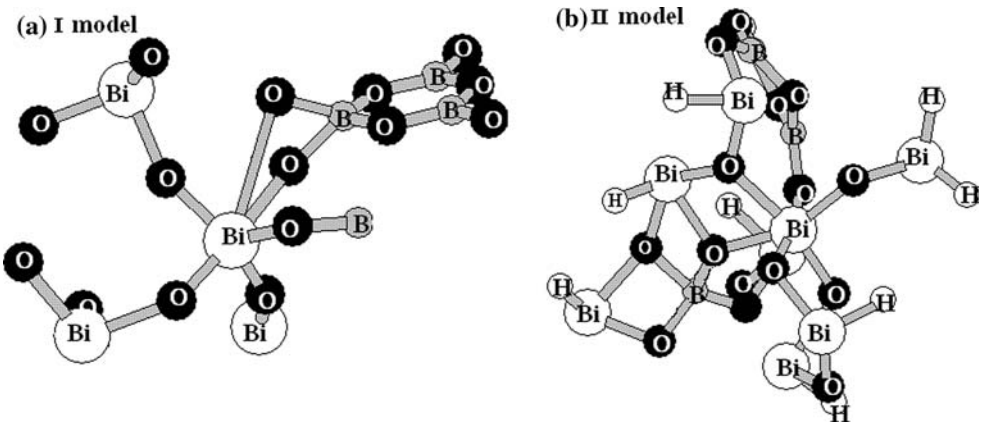

Fig. 2 The optimized structures of two possible models for the $4Bi_2O_3 \cdot B_2O_3$ boro–bismuthate glass used to perform the ab initio (HF/LanL2DZ/ECP) and DFT (B3BW91/CEP-4G/ECP) computations

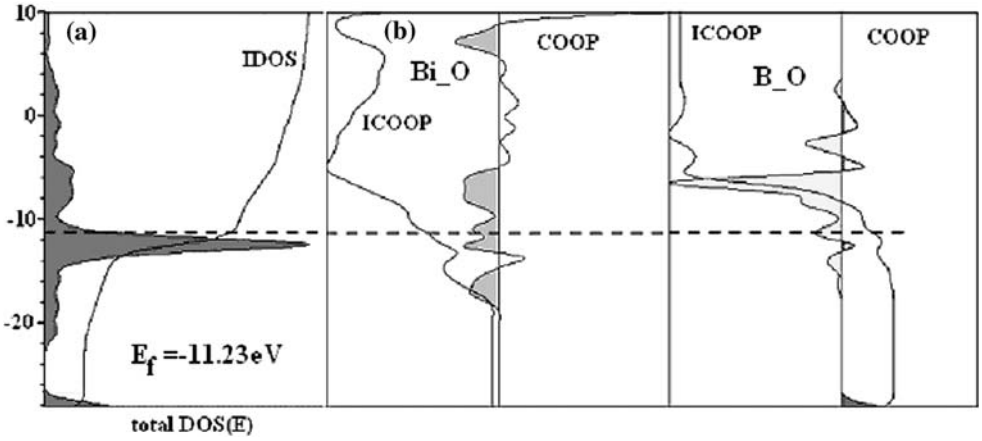

Fig. 3 (**a**) The total density of states plots of $4Bi_2O_3 \cdot B_2O_3$ glass in the energy region from −28 eV and 10 eV. The dotted horizontal line indicates the Fermi level; (**b**) ICOOP(E), COOP(E) curves for all relevant atom–atom interactions in the $4Bi_2O_3 \cdot B_2O_3$ glass

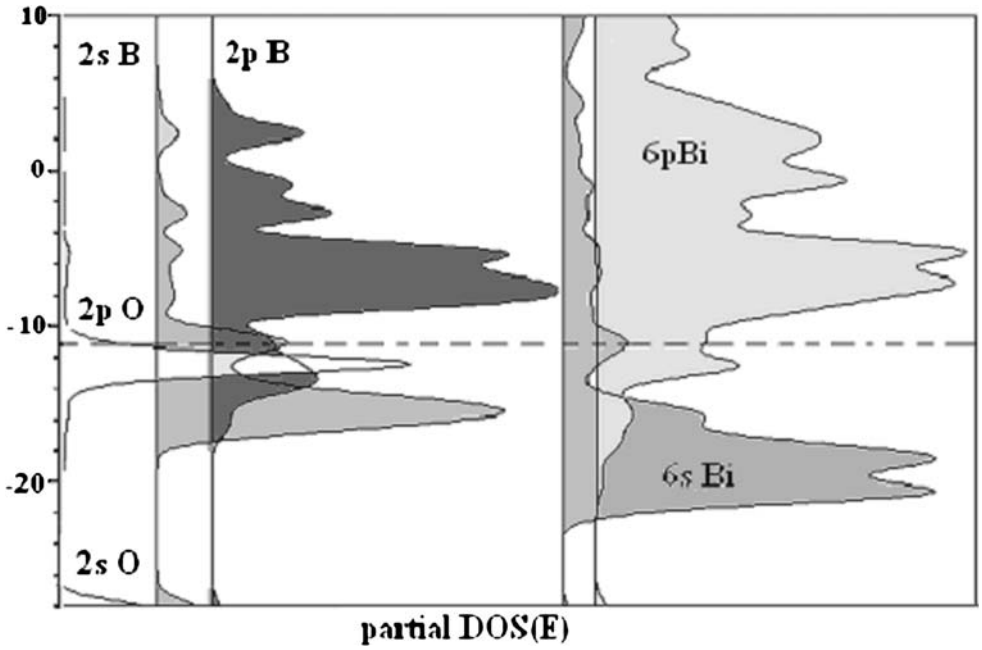

Fig. 4 The partial DOS(E) diagrams of the clusters from the $4Bi_2O_3 \cdot B_2O_3$ glass

silicate glasses (with the O(2s) peak located at about −16.5 eV) [35–38]. This location may be due to the contribution of the nonbridging oxygen atoms present in the glass network [35–38].

The Fermi level is located in the middle of the Van Hove singularities corresponding to the B s-orbital and Bi s-orbital derived states. This is considered an indication that there is an overlap with oxygen orbitals. The Van Hove singularities corresponding to bismuth and boron orbital derived states are cleft suggesting that there are strong boron–oxygen and bismuth–oxygen interactions. This agrees with the results of the ab initio calculations that show the presence of Bi–O and B–O bonds with variable lengths.

We have applied the crystal orbital overlap population (COOP) scheme [37] to analyze the chemical bonds into the two clusters elaborated to model the structure of the $4Bi_2O_3 \cdot B_2O_3$ glass (Fig. 3b). COOP describes the density of bonding and antibonding interaction between specific orbitals at a given energy in solids. Regions with positive COOP contributions are bonding, those with negative COOP contributions are antibonding, and the ones with zero COOP contributions are nonbonding [37]. To determine the overall interaction of two atoms at a given distance, bonding and antibonding contributions are integrated up to the Fermi level.

The integration of the crystal orbital overlap population (ICOOP) curve is maximal below, above, and just at the Fermi level for B–O bonds. The electron filling is optimal for boron–oxygen interaction indicating strong B–O bonding [37].

The valence band consists of the O(2p), B(2s, 2p), and Bi (6s, 6p) hybrids, forming bonding and antibonding states separated by nonbonding bands. The bonding B–O interaction is only slightly weakened by an antibonding region just below the valence band edge while the bonding Bi–O

interaction is located on the top of the conduction band and was found to be very important for the stability of the calculated structural model.

Conclusions

Our results evidence that the Bi^{+3} cations are incorporated in the glass network as [BiO_3] pyramidal, [BiO_6] octahedral, and as distorted [BiO_6] octahedral units. On the other hand a strong distortering effect of Bi_2O_3 on the vitreous B_2O_3 network is demonstrated and this effect increases when the boron cation of the [BO_4] unit is situated in the vicinity of a boroxol ring.

The Van Hove singularities corresponding to bismuth and boron orbital derived states are cleft suggesting that there are strong boron–oxygen and bismuth–oxygen interactions. This explains the results obtained by the ab initio calculations that show diverse Bi–O and B–O bond lengths. The [BiO_6] and [BO_4] structural units that build up the studied glass network have a complex structural role that makes possible the formation of the $4Bi_2O_3 \cdot B_2O_3$ vitreous system.

References

1. Pan A, Ghosh A (2000) J Non-Cryst Solids 271:157. doi:10.1016/S0022-3093(00)00111-3
2. Kityk IV, Imiolek W, Majchrowski A, Michalski E (2003) Opt Commun 219:421. doi:10.1016/S0030-4018(03)01309-9
3. Fu J, Yatsuda H (1995) Phys Chem Glasses 36:211
4. Stehle C, Vira C, Vira D, Hogan D, Feller S, Affatigato M (1998) Phys Chem Glasses 39(2):83
5. Pascuta P, Pop L, Rada S, Bosca M, Culea E (2008) J Mater Sci Mater Electron 19(5):424. doi:10.1007/s10854-007-9359-5
6. Ghosh A (1985) J Chem Phys 102:1385. doi:10.1063/1.468924
7. Pop L, Culea E, Bosca M, Neumann M, Muntean R, Pascuta P, Rada S (2008) J Optoelectr Adv Mater 10(3):619
8. Ghosh A, Chaudhuri BK (1987) J Mater Sci 22:2369. doi:10.1007/BF01082118
9. Rada S, Pascuta P, Bosca M, Culea M, Pop L, Culea E (2008) Vib Spectrosc. doi:10.1016/j.vibspec.2007.12.005
10. Dumbaugh WH (1986) Phys Chem Glasses 27:119
11. Culea E, Pop L, Simon V, Neumann M, Bratu I (2004) J Non-Cryst Solids 337:62. doi:10.1016/j.jnoncrysol.2004.03.104
12. Bishay A, Maghay C (1969) Phys Chem Glasses 10:1
13. Pan A, Ghosh A (2000) J Chem Phys 112:1503. doi:10.1063/1.480717
14. Ghosh A (1989) J Appl Phys 66:2425. doi:10.1063/1.344251
15. Abdeslam C, Chakib A, Mandil A, Tairi A, Ramzi Z, Benmokhtar S (2007) Scr Mater 56:93. doi:10.1016/j.scriptamat.2006.09.025
16. Kondakova OA, Zyubin AS, Dembovsky SA (2003) Solid State Ionics 157:305. doi:10.1016/S0167-2738(02)00226-6
17. Kondakova OA, Zyubin AS, Dembovsky SA (2000) Glass Phys Chem 26:418
18. Laurence RP, Hiller IH (2003) Comput Mater Sci 28:63. doi:10.1016/S0927-0256(03)00057-0
19. Spartan'04, Wavefunction Inc., 18401 Von Karman Avenue, Suite 370 Irvine, CA 92612
20. Frisch MJ, Trucks GW, Schlegel HB, Scuseria GE, Robb MA, Cheeseman JR, Zakrzewski VG, Montgomery JA, Stratmann RE, Burant JC, Dapprich S, Millam JM, Daniels AD, Kudin KN, Strain MC, Farkas O, Tomasi J, Barone V, Cossi M, Cammi R, Mennucci B, Pomelli C, Adamo C, Clifford S, Ochterski J, Petersson GA, Ayala PY, Cui Q, Morokuma K, Rega N, Salvador P, Dannenberg JJ, Malick DK, Rabuck AD, Raghavachari K, Foresman JB, Cioslowski J, Ortiz JV, Baboul AG, Stefanov BB, Liu G, Liashenko A, Piskorz P, Komaromi I, Gomperts R, Martin RL, Fox DJ, Keith T, Al-Laham MA, Peng CY, Nanayakkara A, Challocombe M, Gill PMW, Johnson B, Chen W, Wong MW, Andres JL, Gonzales C, Head-Gordon M, Replogle ES, Pople JA (1998) Gaussian 98 Rev A.5 programme. Gaussian Inc., Pittsburgh, PA
21. Hay PJ, Wadt WR (1985) J Chem Phys 82:270. doi:10.1063/1.448799
22. Gorelsky SI (1999) SWizard. Department of Chemistry, York University: Toronto, ON, http://www.sg-chem.net
23. Brandle M, Rytz R, Calzaferri G (1997) BICON-CEDIT-manual, University of Bern
24. Yang J, Dolg M (2006) J Phys Chem 110B:19254
25. Teng B, Yu WT, Wang JY, Cheng XF, Dong SM, Liu YG (2002) Acta Crystallogr C58:i25. doi:10.1107/S0108270101019643
26. Meera BN, Ramakrishna J (1993) J Non-Cryst Solids 159:1. doi:10.1016/0022-3093(93)91277-A
27. Kharlamov AA, Almeida RM, Heo J (1996) J Non-Cryst Solids 202:233. doi:10.1016/0022-3093(96)00192-5
28. Culea E, Pop L, Simon S, Culea M (2005) J Magn Magn Mater 290–291:1465. doi:10.1016/j.jmmm.2004.11.549
29. Dimitriev Y, Mihailova M (1992) Proceedings of the 16th international congress on glass, Madrid, vol 3, p 293
30. Dwivedi BP, Rahman MH, Kumar Y, Khanna BN (1993) J Phys Chem Solids 54:621. doi:10.1016/0022-3697(93)90242-J
31. Kamistos EI, Karakassides MA, Chryssikos GD (1989) Phys Chem Glasses 306:229
32. Radaev SF, Simonov VI (1992) Sov Phys Crystallogr 37:484
33. Rada S, Culea M, Neumann M, Culea E (2008) Chem Phys Lett 460:196. doi:10.1016/j.cplett.2008.05.088
34. Ispas S, Benoit M, Jund P, Jullien R (2001) Phys Rev B 64:214206. doi:10.1103/PhysRevB.64.214206
35. Muray RA, Ching WY (1987) J Non-Cryst Solids 94:144. doi:10.1016/S0022-3093(87)80267-3
36. Tilloca A, de Leeuw NH (2006) J Phys Chem B 110:25810. doi:10.1021/jp065146k
37. Hughbanks T, Hoffmann R (1983) J Am Chem Soc 105:3528. doi:10.1021/ja00349a027
38. Rytz R, Hoffmann R (1999) Inorg Chem 38:1609. doi:10.1021/ic981075v